Eur. Phys. J. D **43**, 73–76 (2007)
DOI: 10.1140/epjd/e2007-00100-3

THE EUROPEAN PHYSICAL JOURNAL D

Electron-ion-coincidence spectra for deep inner-shell excited rare-gas clusters

H. Murakami[a], H. Iwayama, K. Nagaya, Y. Ohmasa, and M. Yao

Department of Physics, Kyoto University, 606-8502 Kyoto, Japan

Received 25 July 2006 / Received in final form 17 October 2006
Published online 24 May 2007 –

Abstract. Electron-Ion-Coincidence (EICO) and Multiple-Ion Coincidence Momentum Imaging (MICMI) measurements were carried out for deep inner-core excited rare-gas clusters. From MICMI measurements, momentum distributions and time-of-flight (TOF) spectra of daughter ions were obtained for the number of coincident signals, $N_{\rm coin}$, up to 8. The TOF spectra for $N_{\rm coin}$ larger than 2 indicate that only singly-charged ions are the products of Coulomb explosion. The observed fragmentation pattern and the momentum distribution of singly-charged daughter ions reveal that the heavier ions have smaller momentum than the monomer ions. This suggests that the heavier ions are produced in the central part of clusters where the Coulomb forces from the surrounding ions are more effectively canceled out. All these results are consistent with the site-dependent decay process predicted recently by us for Kr clusters.

PACS. 36.40.-c Atomic and molecular clusters – 36.40.Qv Stability and fragmentation of clusters – 36.40.Wa Charged clusters

1 Introduction

Tremendous efforts have been devoted to study rare-gas clusters, because they belong to the simplest clusters that can provide basic information on cluster science. Recently, not only the size-dependent but also site-dependent properties have been studied experimentally by core hole excitation [1]. When a core hole is generated within a neutral cluster by absorbing an X-ray photon, the cluster is changed to a multiply-charged state by Auger cascade decay, and then the charges are separated to different atomic sites within the clusters, resulting in the Coulomb explosion. In particular, fragmentation processes of $2p$-excited argon clusters have been well studied by coincidence experiments such as photoelectron-photoion-photoion-photoion coincidences (PEPIPIPICO) [2–4]. Compared with these soft X-ray experiments, deep inner-shell spectroscopy of rare-gas clusters has been rather limited, because the absorption cross-section of hard X-ray is considerably small.

The first Electron-Ion-COincidence (EICO) measurements by utilizing hard X-ray were done by our group [5] for Kr clusters. We found that dominant ionic species stemming from small neutral clusters are highly-charged monomer ions, while for medium size clusters singly-charged monomer ions become the most abundant. Then the fraction of singly-charged dimers and subsequently that of trimers increase with increasing cluster size. We have interpreted the characteristic size-dependence of the relative abundance of daughter ions by assuming site-dependent decay processes: when the core hole is generated on the cluster surface, the proliferated holes due to the vacancy cascade are strongly localized within the X-ray absorbing atom, while the charges are separated to surrounding atoms when the X-ray absorption takes place inside the cluster. This interpretation is consistent with the idea of a chromophoric core proposed by Haberland et al. [6], and also with the Interatomic Coulombic Decay (ICD) theoretically predicted some years ago [7] and experimentally proved lately [8,9].

In the present work, we have extended the EICO measurements to Ar and Ne clusters, and we have developed a Multiple-Ion Coincidence Momentum Imaging (MICMI) technique [10], from which the momentum distribution of daughter ions can be recorded as well as time-of-flight (TOF) spectra obtained for the number of coincident signals, $N_{\rm coin}$, up to 8. In this paper, we report some representative results of the EICO and MICMI measurements for Ar clusters, and discuss the charge migration dynamics and Coulomb explosion mechanism as a function of the average cluster size $\langle N \rangle$ and the number of charges z_0 induced by the core excitation and vacancy cascade.

2 Experiment

The experiments were performed at the beam line BL37XU installed in SPring-8, where the high-brilliance

[a] e-mail: mura00@scphys.kyoto-u.ac.jp

X-ray emitted from the undulator was monochromatized by a Si(111) double-crystal. The photon flux of the X-ray beam was about 1.0×10^{13} photons/s during our measurements. The measurements were carried out at a photon energy of 14.08 keV.

Neutral clusters were produced in a supersonic expansion of Ar gas through a cylindrical nozzle with a diameter of 60 μm. The nozzle was mounted on top of a cryostat which can be operated with liquid nitrogen. A gas jet created in the expansion chamber was introduced to an analyzing chamber through a conical skimmer with an aperture of 1 mm and crossed with the X-ray beam. The pressure in the analyzing chamber was typically 10^{-4} Pa during the experiment. The cluster size was varied by choosing appropriate expansion parameters: the stagnation pressure was changed from 1 to 9 bars and the nozzle temperature was kept at 130 K. The average cluster size was estimated from a mass spectrum obtained using electron impact ionization, and our result agreed well with a relation derived by Karnbach et al. [11] between the mass and the scaling parameter Γ^* [12]. Further experimental details are described elsewhere [13].

In the EICO measurements, electrons and ions were generated by photoionization of the neutral cluster beam and extracted by a static field in opposite directions. Then the ions were detected by a channeltron after passing through a flight tube, which works as a Wiley-McLaren type time-of-flight (TOF) mass spectrometer, and the electrons were immediately detected by another channeltron. The electron signal was fed to a Time-to-Amplitude-Converter (TAC) as a start pulse, and the ion signal as a stop pulse. The TOF spectrum was recorded by a Multi-Channel-Analyzer (MCA).

An experimental setup for the MICMI measurements was the same as that for the EICO measurements except that the ion detector was replaced by a position and time sensitive multi-hit MCP delay-line detector system (RoentDek DLD40 and TDC8). Moreover, we set a slit with 1mm width behind the skimmer in order to limit the ionization range, which improved the resolution of TOF spectra compared with that of EICO measurements. Octuple coincidence spectra of daughter ions were recorded for an electron pulse. The detection efficiency was estimated to be about 35%. False-coincidence events were carefully removed from raw data, and both the TOF spectrum and the image on the Position Sensitive Detector (PSD) were sorted by the number of coincidence events, $N_{\rm coin}$. Further details on the MICMI technique will be published elsewhere [10].

3 Result

Figure 1 shows EICO spectra of Ar clusters with various sizes ($\langle N \rangle \leq 300$). For comparison, EICO spectra for Ne and Kr clusters with $\langle N \rangle \sim 300$ are also displayed. Here contributions from uncondensed atoms in the cluster beams were subtracted except for (b). The atomic fraction of uncondensed atoms is ∼35% for Kr, and ∼20% for Ar

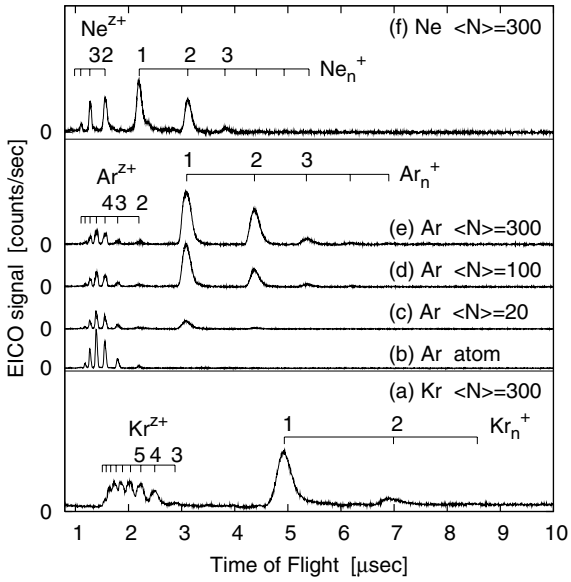

Fig. 1. Representative EICO spectra of (a) Kr, (c)-(e) Ar and (f) Ne clusters; $\langle N \rangle$ is average cluster size; (b) is the EICO spectrum of atomic Ar. The photon energy is 14.50 keV for Kr and 14.08 keV for Ar and Ne.

and Ne clusters, which was determined by mass spectrometry using electron impact ionization. In the EICO spectra of Ar clusters, a series of narrow peaks due to multiply-charged monomer ions, Ar^{z+} ($z = 2-8$), are seen below 2.5 μs, and broad peaks due to the singly-charged ions, Ar_n^+ ($n = 1-4$), above 2.8 μs.

It is believed that small rare-gas clusters have a multilayer icosahedral structure [14]. For Kr clusters, multiply-charged ions exhibits nearly the same $\langle N \rangle$ dependence as the fraction of atoms existing in the first outer shell of icosahedrons [5]. In the present case the fraction of Ar^{z+} ($z = 2-8$) decreases with $\langle N \rangle$, but it is smaller than the fraction of surface atoms [13]. The relative intensity of the peaks corresponding to Ar^{z+} ($z = 2-8$) changes very little with $\langle N \rangle$, and the average number of the induced charges, $\langle z_0 \rangle$ remains 4.6. On the other hand, the Ar_n^+ peaks grow remarkably with increasing $\langle N \rangle$. Compared with Kr clusters, the intensity of the dimer ions relative to that of monomers is much larger for Ar clusters. The dimer ions become dominant for larger $\langle N \rangle$ [13]. The dominance of Ar_2^+ was also found by Rühl et al. in their soft X-ray coincidence measurements but for smaller size [2–4].

Figure 2 shows the TOF spectra recorded by the MICMI measurements (hereafter abbreviated as MICMI-TOF) for Ar clusters with $\langle N \rangle = 200$. The spectra are sorted by the number of coincident signals, $N_{\rm coin}$, from 1 to 8. Multiply-charged ions $Ar^{z+}(z = 2-8)$ (below 2.4 μs) and singly-charged ions Ar_n^+ ($n = 1-4$) (above 2.9 μs) are observed for $N_{\rm coin} = 1$. Because the intensity of $Ar^{z+}(z = 2-8)$ is substantially damped for $N_{\rm coin} \geq 2$, the multiply-charged ions are not considered to be produced by the Coulomb explosion. This is consistent with the narrow line width and also with the fact that the charge distribution within the multiply-charged ions hardly changes

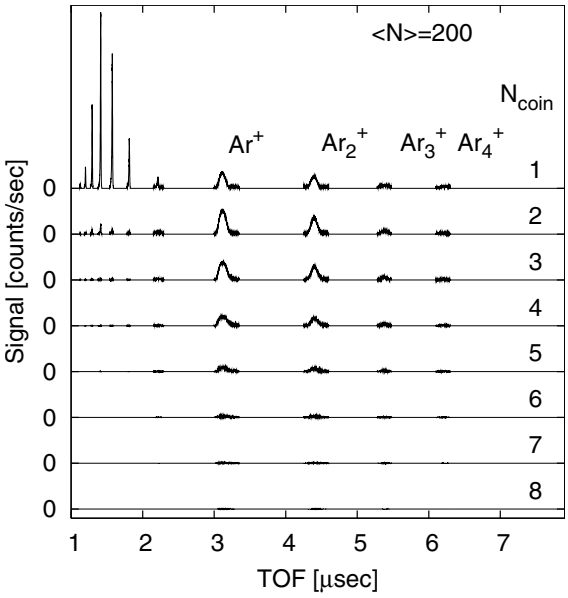

Fig. 2. MICMI-TOF spectra for Ar clusters with $\langle N \rangle = 200$. The spectra are sorted by the number of coincident signals, $N_{\rm coin}$, from 1 to 8. Photon-energy is 14.08 keV.

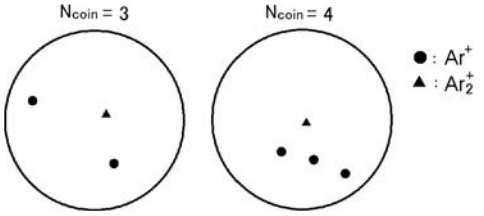

Fig. 3. A typical snap shot of the PSD image for $N_{\rm coin} = 3$ and $N_{\rm coin} = 4$. The diameter of PSD is 40 mm.

with $\langle N \rangle$ in the TOF spectra for EICO and MICMI measurements. By contrast, the singly-charged ions are detected in a wide range of $N_{\rm coin}$ and their relative abundance changes with $N_{\rm coin}$, indicating that they are products of Coulomb explosion. One may infer from Figure 2 that the singly-charged monomer is the major product for small $N_{\rm coin}$ and the dimers becomes more important with increasing $N_{\rm coin}$.

Indeed by counting all the individual events, it has been proved for $N_{\rm coin} = 3$ that the most frequent decay channels are $Ar^+ + Ar^+ + Ar_2^+$ and $Ar^+ + Ar^+ + Ar^+$, and the next important channels are $Ar^+ + Ar_2^+ + Ar_2^+$ and $Ar_2^+ + Ar_2^+ + Ar_2^+$. All these channels were observed in the PEPIPIPICO spectra [4] for $2p$ excited Ar clusters with $\langle N \rangle = 175$, though $Ar_2^+ + Ar_2^+ + Ar_2^+$ was the most frequent in the soft X-ray experiment. For $N_{\rm coin} = 4$, $Ar^+ + Ar^+ + Ar^+ + Ar_2^+$ and $Ar^+ + Ar^+ + Ar_2^+ + Ar_2^+$ take place frequently.

In the present experiment, the momentum distribution can be deduced from the detection image on the PSD and the TOF. Figure 3 displays a typical snap shot of the PSD image for $N_{\rm coin} = 3$ (a) and $N_{\rm coin} = 4$ (b). It should be noted that in both cases the dimer ion hits the central part of PSD, while the monomers are distributed in the off center part.

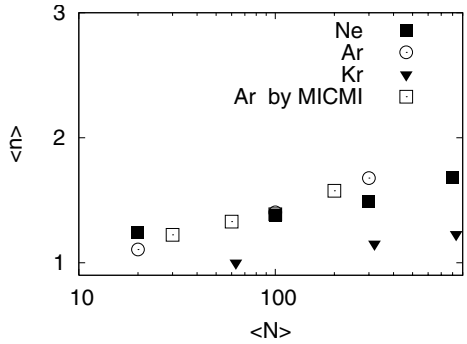

Fig. 4. Average number of atoms per charge, $\langle n \rangle$, is plotted against $\langle N \rangle$ for Ne, Ar and Kr. For Ar clusters $\langle n \rangle$ estimated from MICMI-TOF spectra are also plotted.

Table 1. A relation between the number of coincident event, $N_{\rm coin}$, and the average of the initially generated charges in clusters, $\langle z_0 \rangle_{\rm coin}$, for Ar clusters.

$N_{\rm coin}$	1	2	3	4	5	6	7	8
$\langle z_0 \rangle_{\rm coin}$	4.3	4.6	5.0	5.4	6.0	6.7	7.4	8.0

4 Discussion

In this section we restrict ourselves to discussion of the singly-charged daughter ions, because the multiply-charged ions exhibit considerably different $\langle N \rangle$ and $N_{\rm coin}$ dependences, as seen in Figures 1 and 2. In Figure 4 the average number of atoms per charge, $\langle n \rangle$, is plotted against $\langle N \rangle$ for Ne, Ar and Kr. Here $\langle n \rangle$ is calculated by

$$\langle n \rangle = \frac{\sum_n n I_n}{\sum_n I_n}, \tag{1}$$

where I_n is the integrated intensity of the peak in the EICO spectra. Detailed information on Ne clusters and larger Ar clusters will be described elsewhere [13]. Since the charges initially generated by an inner core excitation are strongly localized, $\langle n \rangle$ is expected to serve as a measure of charge separation distance. As seen in Figure 4, $\langle n \rangle$ increases with $\langle N \rangle$ for all the elements. Compared among the rare gas elements, $\langle n \rangle$ for Kr clusters is appreciably smaller than that of Ar and Ne clusters.

Since the number of charges, z_0, initially induced by photo-absorption depends on the element (i.e. $\langle z_0 \rangle = 2.7$ for Ne, 4.6 for Ar and 6.2 for Kr clusters [13]), we should first discuss the dependence of $\langle n \rangle$ on z_0 by utilizing the fact that z_0 generally increases with $N_{\rm coin}$. Following a prescription described in reference [10], a relation between the average of z_0, $\langle z_0 \rangle_{\rm coin}$, and $N_{\rm coin}$ is presented in Table 1 for Ar clusters. In this estimation we have assumed that the distribution of z_0 within the clusters is the same as that of isolated atoms, because the Auger processes occurs essentially within an X-ray absorbing atom [15]. We

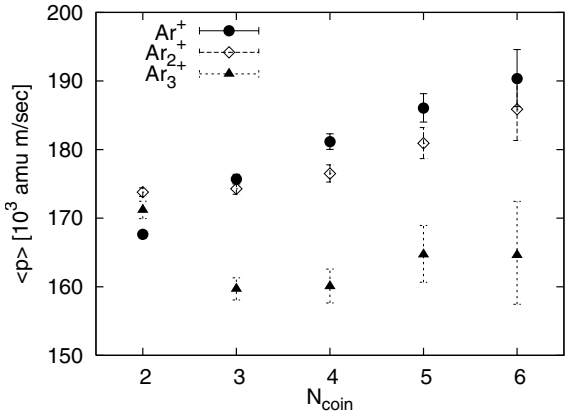

Fig. 5. Average momentum of fragment ions Ar_n^+ ($n = 1-3$) for $\langle N \rangle = 200$. Statistical errors are denoted by bars.

have also assumed that the detection of different ions can be treated as independent events. The open squares in Figure 4 denotes $\langle n \rangle$ estimated from MICMI-TOF when $N_{\rm coin}$ changes from 2 to 6 (i.e. when $\langle z_0 \rangle_{\rm coin}$ changes from 4.6 to 6.7). It should be noted that the range is quite small, indicating that the dependence of $\langle n \rangle$ on z_0 is unimportant.

We should be still careful to make a comparison among the elements, because we cannot overlook a possibility that, even if stable cluster ions are formed, they may be dissociated on the Coulomb explosion. Therefore, $\langle n \rangle$ should be regarded as a minimum size of stable ions. Nevertheless, one may conclude that Kr clusters have a more localized character than the lighter elements, because the van der Waals potential of Kr is much deeper and hence Kr clusters are expected to more stable [16].

Figure 5 shows the average momentum $\langle p \rangle$ of daughter ions Ar_n^+ ($n = 1-3$) as a function of $N_{\rm coin}$. Here $p = \sqrt{p_x^2 + p_y^2 + p_z^2}$ and the momenta of the fragment ions immediately after the Coulomb explosion, p_x, p_y, p_z, can be derived from the detected position on the PSD and TOF by a well-known method [17]. As $N_{\rm coin}$ increases, the $\langle p \rangle$ of singly-charged monomer ions increases, while the $\langle p \rangle$ of trimer ions remains small. Because the total Coulomb energy and hence the total kinetic energy release increase with $N_{\rm coin}$, the present result for trimers looks contradictory. However, the apparent discrepancy can be resolved by considering that the heavier ions are produced in the central part of clusters where the Coulomb forces from the surrounding ions are more effectively canceled out due to the higher symmetry. This is fully consistent with the site dependent decay process suggested for Kr clusters [5] and also consistent with the formation of a chromophoric core. Since the chromophoric core has linear conformation because of the directional character of the empty p-orbital [6], it may not be stable enough to survive after the Coulomb explosion unless the cluster size is sufficiently large. This may be a reason for the observed monotonous increase of $\langle n \rangle$ with $\langle N \rangle$.

5 Conclusion

Electron-Ion-Coincidence (EICO) and Multiple-Ion Coincidence Momentum Imaging (MICMI) measurements were carried out for deep inner-core excited rare-gas clusters, especially for argon clusters. The average number of atoms per charge, $\langle n \rangle$, estimated from the EICO spectra increases with increasing the cluster size. The comparison of $\langle n \rangle$ among Ne, Ar and Kr reveals that Kr clusters have more localized character than the lighter elements. In the TOF spectra for MICMI measurements multiply-charged daughter ions were observed mainly for $N_{\rm coin} = 1$, where $N_{\rm coin}$ is the number of coincident signals, while singly-charged ions were observed for $N_{\rm coin} \geq 2$, indicating that only singly-charged ions are the products of Coulomb explosion. From the fragmentation pattern of the Coulomb explosion and the momentum distribution of singly-charged daughter ions, it is concluded that the heavier ions have much smaller momentum than the monomer ions, suggesting that the heavier ions are produced in the central part of clusters where the Coulomb forces from the surrounding ions are more effectively canceled out due to the higher symmetry. All these results are consistent with the site-dependent decay process predicted recently by us for Kr clusters [5].

The authors are grateful to Messrs H. Kajikawa and Y. Nishimori for their collaboration in carrying out experiments. This work is supported by the Grant-in-Aid for the 21st Century COE "Center for Diversity and Universality in Physics" from the Ministry of Education, Culture, Sports, Science and Technology (MEXT) of Japan. This work is also supported by the Grant-in-Aid for Scientific Research from the JPSJ (No. 12554013, 15651044, 16201021, 18710087).

References

1. E. Rühl, Int. J. Mass. Spectr. **229**, 117 (2003)
2. E. Rühl et al., J. Chem. Phys. **95**, 6544 (1991)
3. E. Rühl et al., Z. Phys. D **31**, 245 (1994)
4. E. Rühl et al., Surf. Rev. Lett. **3**, 557 (1996)
5. K. Nagaya et al., J. Phys. Soc. Jpn **75**, 114801 (2006)
6. H. Haberland et al., Phys. Rev. Lett. **67**, 3290 (1991)
7. L.S. Cederbaum et al., Phys. Rev. Lett. **77**, 4778 (1997)
8. R. Santra et al., Phys. Rev. B **64**, 245104 (2001)
9. G. Öhrwall et al., Phys. Rev. Lett. **93**, 173401-1 (2004)
10. H. Iwayama et al., J. Chem. Phys. **126**, 024305 (2007)
11. R. Karnbach et al., Rev. Sci. Instrum. **64**, 2838 (1993)
12. O.F. Hagena, W. Obert, J. Chem. Phys. **56**, 1793 (1972)
13. H. Murakami et al., J. Chem. Phys. (accepted)
14. J. Farges et al., J. Chem. Phys. **84**, 3491 (1986)
15. T. Hayakawa et al., J. Phys. Soc. Jpn **69**, 2039 (2000)
16. e.g. W.A. Harrison, *Electronic Structure and the Properties of Solids* (San Francisco, Freeman, 1980), Chap. 12
17. R. Dörner et al., Phys. Rep. **330**, 95 (2000)